Medical & Biological Engineering & Computing (2023) 61:45–59
https://doi.org/10.1007/s11517-022-02687-w

ORIGINAL ARTICLE

# Multiclass tumor identification using combined texture and statistical features

**Ghazanfar Latif[1,2] · Abul Bashar[3] · D. N. F. Awang Iskandar[4] · Nazeeruddin Mohammad[1] · Ghassen Ben Brahim[1] · Jaafar M. Alghazo[5]**

Received: 30 April 2022 / Accepted: 2 October 2022 / Published online: 2 November 2022


**Abstract**
Early detection and diagnosis of brain tumors are essential for early intervention and eventually successful treatment plans leading to either a full recovery or an increase in the patient lifespan. However, diagnosis of brain tumors is not an easy task since it requires highly skilled professionals, making this procedure both costly and time-consuming. The diagnosis process relying on MR images gets even harder in the presence of similar objects in terms of their density, size, and shape. No matter how skilled professionals are, their task is still prone to human error. The main aim of this work is to propose a system that can automatically classify and diagnose glioma brain tumors into one of the four tumor types: (1) necrosis, (2) edema, (3) enhancing, and (4) non-enhancing. In this paper, we propose a combined texture discrete wavelet transform (DWT) and statistical features based on the first- and second-order features for the accurate classification and diagnosis of multiclass glioma tumors. Four well-known classifiers, namely, support vector machines (SVM), random forest (RF), multilayer perceptron (MLP), and naïve Bayes (NB), are used for classification. The BraTS 2018 dataset is used for the experiments, and with the combined DWT and statistical features, the RF classifier achieved the highest average accuracy whether for separated modalities or combined modalities. The highest average accuracy of 89.59% and 90.28% for HGG and LGG, respectively, was reported in this paper. It has also been observed that the proposed method outperforms similar existing methods reported in the extant literature.

**Keywords** Multiclass tumor classification · Statistical features · Texture features · Glioma tumor · Tumor detection · Magnetic resonance imaging

## 1 Introduction

During their lifetime, human beings may face several types of diseases which differ in terms of severeness and the importance of early-stage detection and type of treatment. Brain tumor falls under the category of dangerous diseases with a significantly high mortality rate, which is better treated if detected at an early stage. Reports are showing that prompt and precise detection of such disease and eventual subsequent efficient treatment will most likely increase patients' life expectancy and/or full recovery [1].

The process of tumor detection and diagnosis is usually performed by experienced pathologists who will be looking for anomalies and well-defined features in the collected histological slides and tissues. Following this analysis, pathologists may classify patients' samples as being either normal vs. tumor, metastatic vs. primary, or the grade/degree of malignancy of the tumor, or the type of the tumor [2]. The diagnosis process is usually done manually and suffers from several challenges such as the number of cases that experts need to analyze and eventually file a report in a timely manner, the human

✉ Ghazanfar Latif
glatif@pmu.edu.sa

1 Computer Science Department, Prince Mohammad Bin Fahd University, Al Khobar, Saudi Arabia

2 Université du Québec a Chicoutimi, 555 boulevard de l'Université, Chicoutimi, Saguenay, QC G7H2B1, Canada

3 Department of Computer Engineering, Prince Mohammad Bin Fahd University, Al Khobar, Saudi Arabia

4 Faculty of Computer Science and Information Technology, Universiti Malaysia Sarawak, Kota Samarahan, Malaysia

5 Department of Electrical and Computer Engineering, Virginia Military Institute, Lexington, VA 24450, USA

error in identifying some of the features, or the subjectivity in categorizing the tumor grade [3]. It was reported that these challenges are only expected to increase and become more challenging in the future [1]. Therefore, more and more interest and efforts have been shifted towards using computer-aided diagnostic tools during the tumor detection and classification process [4]. Thus, physicians being supported with CAD tools are more likely to make correct diagnoses and classifications compared to relying on self-visual analysis.

Recently, artificial intelligence has proven its effectiveness and success in image classification through its computer vision and machine learning subfields. The creation and rapid development of various machine learning techniques in terms of their ability in classifying medical images have contributed to the high adoption of CAD techniques during medical diagnosis. These techniques include the deep learning-based models, which have contributed to the significant improvement of classification accuracy [5].

The diagnosis and classification of the glioma tumors into either of four classes face many challenges. These challenges could be categorized in two categories. The first category consists of the lack of resource availability; in terms of experts and highly qualified individuals. These are being outnumbered with the number of cases that need to be analyzed and diagnosed. The second category is due to the nature and the size of the targeted classes (which are four in this problem — edema, necrosis, enhancing tumor, and non-enhancing tumor) which are defined based on the intra-tumoral structures. These intra-structure-based four classes offer biological interpretation of the annotated image patterns. This complexity manifests in the high correlation between the characteristics and pixels of the MR images making the distinction between the various types of tumor very difficult and prone to errors, when manual processing is applied.

Due to the time-consuming process of diagnosing glioma tumors by highly qualified trained individuals, the number of patients that can be processed in a given certain time is limited. Thus, the diagnosis process is only done for patients with suspected tumors which means that the patient has already displayed symptoms. This does not help in the quest for early diagnosis. In addition, since the process is prone to human errors, a misdiagnosis may be possible which results in psychological effects for the patients when being misdiagnosed with glioma tumors. Therefore, if it is possible to develop a system that can process the scans of thousands of patients daily and be able to accurately diagnose tumors, then such a system will help and aid in the early diagnosis of tumors not only for patients who have displayed symptoms but for any patients that have taken scans for any other reason. This would aid in having patients taking scans during their annual check-ups, and the automated system will have the computing power to process the vast number of patients. Such an automated system which is able to accurately classify various types of glioma tumors does not restrict its use and application to the diagnosis phase but also can be utilized during the planning for the treatment phase, for instance, during the radiotherapy treatment. Also, with this type of disease, multiple opinions from different experts are always sought to confirm the diagnosis. This is, in most of the time, very hard to achieve in due time due to the non-availability of medical experts who will be analyzing the MR images. The proposed automated systems with high accuracy level could serve as a second opinion to the diagnosis phase which will result in speeding up the actions needed in terms of type of treatment and actions.

The aim of this paper is to propose a system that can automatically diagnose glioma tumors using MRI images (MICCAI BraTS 2018 Dataset) and will also be able to classify with high accuracy whether the tumor falls into any of the four specified classes. The first novelty of our proposed approach lies in generating MRI image features from two different domains, namely, the spatial domain and the frequency domain. The statistical features utilize the spatial information in the images, and we get 52 features which describe the various statistical aspects of the image. The DWT approach captures the frequency domain information and provide us with another 100 features related to the image texture. The unique combination of these features (152 in total) provides a creative aspect to our proposed methodology. Secondly, our approach uses the popular ML classifiers for performing the multiclass classification (as opposed to binary classification, tumorous/non-tumorous classes) of MRI images into 4 classes, namely, (1) necrosis, (2) edema, (3) enhancing, and (4) non-enhancing. Lastly, the choice of the supervised ML classifiers has been made on multiple criteria: ease of implementation (for NB), the generalization of the approach (for MLP), handling of data variability (for SVM), and improved classification accuracy (for RF). The novelty and applicability of our approach are later reflected in the performance results which show that the proposed model achieves better accuracy compared to the existing benchmarking models.

This paper is organized as follows. Section 2 reports the most recent work related to the classification of brain tumors as well as the various techniques being used. Section 3 describes the details of the methodology proposed in this research work. Section 4 illustrates the experiments and discussion of the reported results. Section 5 concludes this work. Section 6 lists all references used.

## 2 Literature review

In this section, we present a detailed review of the research that has been performed in the area of multiclass glioma tumor identification using machine learning approaches. The review presents both a historical perspective and the recent advancements that are reported in the extant literature. In general, we discuss the approaches from the perspective of the types of features used (texture-based or statistical-based), machine learning (ML) classification techniques used, datasets worked on, the results achieved, and their merits and drawbacks. This helps us in identifying the research gap.

In one of the early works by Zacharaki et al. [6], Gabor features were extracted from the MRI images of the brain. These features were given as input to the SVM classifier to identify the presence of tumors in the patient. They were able to successfully identify 5 different classes of brain tumors with a multiclass classification accuracy of 85%. However, the drawback of this research was that the training of the classifier was done with only 98 MRI images, which is considered to be too low. This is also reflected in the low classification accuracy achieved in this study. In another work by Jayachandran et al. [7], an SVM classifier was used but with another image, a feature termed co-occurrence matrices. This approach provided a relatively high classification accuracy of 96.8% by utilizing a larger dataset of MRI brain images (442 images). However, this approach only catered to texture-based features, which could have been augmented with more features from the statistical domain. Still working with the popular SVM classifier, Bahadure et al. [8] were able to achieve similar classification accuracy (96.5%) using the Berkeley wavelet transform (BWT) features on a DICOM and Brain Web datasets consisting of 22 and 44 brain MRI, respectively. The versatility of the approach was tested on two different datasets; however, the small size of the dataset still is a concern for the proof of concept.

In a review paper from Iqbal et al. [9], a comparison of various ML classifiers was presented in the context of glioma identification and classification using brain MRI images (summarizing about 106 research papers). The paper also enlists the various prominent texture-based approaches and compares their merits and drawbacks. The details of popular datasets used and their relevance to the research domain are aptly presented; however, considering the recent advances in this field, the paper may already be outdated. Sengupta et al. [10] have again tested the SVM classifier but with statistical features of the MRI images. They have achieved an accuracy of 96.3% on their indigenous dataset consisting of only 66 MRI images. The accuracy was achieved by utilizing a smaller number of features, but the details of the image definitions were not properly made aware to the readers. On the other hand, Gupta et al. [11] have experimented with standard datasets (BRATS and JMCD) to provide a proof of concept for their approach based on the gray-level co-occurrence matrices (GLCM) which represent the texture-based features of images. The noteworthy point here is that they have achieved a higher accuracy of 97.13% through a comparative study of three ML classifiers, which are SVM, KNN, and NB. However, the reason for choosing these classifiers is not properly justified, as well as the method in which they reduced the number of features to use in their experiment.

In remarkable research by Gilanie et al. [12], both the texture-based features (Gabor) and statistical-based features (entropy, kurtosis, etc.) were utilized with the SVM classifier on the Harvard Medical School Dataset. The classification accuracy was significantly very high (99.6%); however, the results presented were scattered and not properly summarized. Bhatele et al. [13] and Jena et al. [14] have based their experiments on the BraTS dataset and achieved similar classification accuracy (97%) by employing an ensemble classifier with hybrid features and five different ML classifiers (SVM, KNN, DT, RF, and ensemble), respectively. Similar results were also achieved by Oksuz et al. [15] by using SVM and KNN classifiers on fused features. The MRI dataset they used (Figshare) consisted of about 3000 images; however, it is not one of the standard datasets which makes it difficult to compare their results with other approaches. Latif et al. used multilayer perceptron (MLP) for binary classification of tumorous images of the BraTS dataset with good accuracy [16]. The authors also performed multiclass classification on the same dataset using different classifiers such as MLP, NB, and RF. The RF classifier generated better results than MLP in their experiments [17].

During the review process, some papers dealt with using deep learning (DL) approaches, in contrast to those approaches that use manual feature extraction techniques with traditional ML classifiers. The popular approach in this category is the convolutional neural networks (CNN), which automatically extract features from the MRI images and then perform classification with their in-built neural network (NN) classifier. DL approaches are known for good image classification accuracy. So, these approaches are applied to MRI as well [18]. However, DL approaches need a relatively large set of images for training deep neural networks, but the medical imaging datasets are considerably small. So, researchers tried to combine DL with traditional approaches. For example, CNN features are combined with the SVM features for MRI classification [19–21]. The main goal of this research is to explore and analyze how far we can go to achieve higher glioma tumor classification rates using the better selection of the features along with the well-known standard classifiers, instead of using the DL methods.

Based on the above review, we propose our approach which combines both the texture-based features and statistical-based features for improved classification performance.

Discrete wavelet transform (DWT) is used for generating the texture-based features, whereas the statistical-based features include mean, entropy, kurtosis, etc. We have also used a standard BRATS 2018 dataset [22] and achieved an accuracy of 90.28% (as will be shown in the results section later).

## 3 Methodology

In the first stage, features were extracted from the extracted brain part of the MR image by applying an ensemble feature set from all four MRI modalities. Since tumor parts can have multiple classes, binary classification was initially performed with different classifiers including SVM, MLP, RF, and NB to classify the MR images into tumorous and non-tumorous images. In the next step, the same combined texture (DWT) and statistical features are used followed by the use of well-known classifiers (SVM, MLP, RF, and NB) to classify glioma tumorous images into four classes, i.e., necrosis, edema, enhancing, and non-enhancing. A total of 152 features for each MR image modality were extracted. The proposed combined texture (DWT) and statistical feature-based technique consist of various stages, which are shown in Fig. 1.

Figure 1 details the proposed methodology in this work. DWT and statistical features are extracted for the four modalities. The combined features are then input to the well-known classifiers to classify the images into one of the four classes.

### 3.1 Dataset description

The dataset used in the brain tumor segmentation is MICCAI BraTS 2018 Dataset [22]. The MICCAI BraTS 2018 specialize in testing the different strategies used in the segmentation of brain tumors in multimodal. BraTS 2018 focuses on the MRI method in surgeries; they concentrate on the segmentation of brain tumors specifically glioma tumors and provide images in four different modalities. Figure 2 shows the samples of the four different brain MRI modalities.

- T1: this modality has a small echo and repetition time. T1 provides a nice image contrast for the various healthy tissues inside the brain, i.e., gray matter, cerebrospinal fluid, and white matter.
- T2: it has a long time of echo and repetition time but slow image acquisition. It provides good contrast for the tumor surrounding tissues (edema).

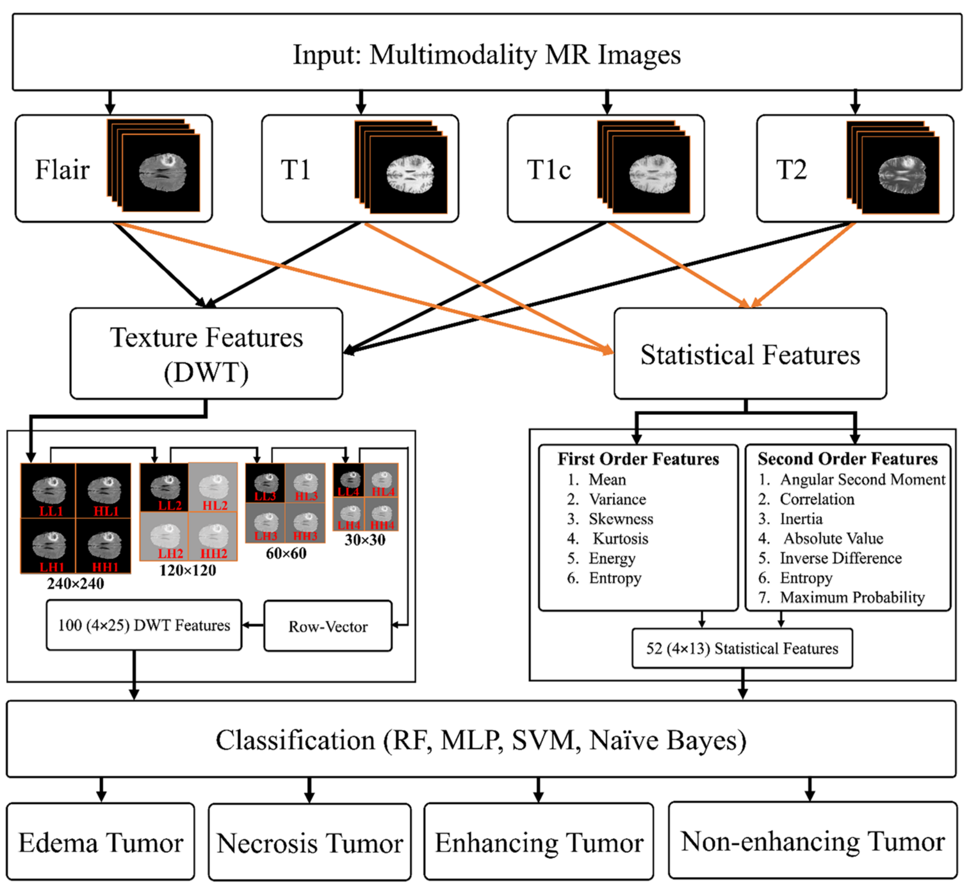


**Fig. 1** Proposed combined texture and statistical feature-based glioma tumor classification

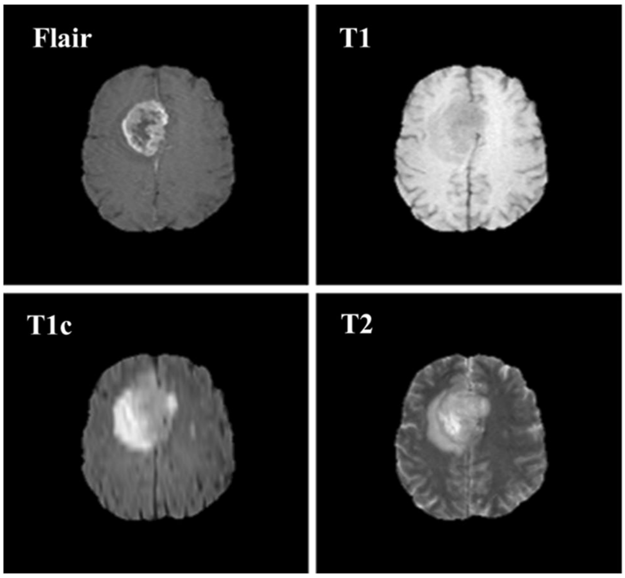


**Fig. 2** Pictorial view of brain MR image modalities

- T1c: it is the same as T1, but a contrast agent is applied to enhance the contrast.
- Flair: it is used to nullify the signal from the fluid, suppress the effect of cerebrospinal fluid (CSF), and bring out the periventricular hyperintense lesion.

For the experiments, a total of 65 cases of data have been used consisting of 39 HGG and 26 LGG. The total number of MR images is 40,300 images. Data exists for all four modalities in the dataset for both HGG and LGG. Figure 3 shows a sample of multiclass glioma labels with different tumor types. The image label shows (A) whole tumor, (B) tumor core, (C) enhancing tumor, and (D) combined all tumor types.

## 3.2 Proposed combined texture and statistical features

A careful selection of beneficial features is necessary for the successful categorization of brain tumor images. The feature extraction process helps in diminishing the dimensionality of brain tumor images into a succinct set of valuable features. A good set of features, which are given as input to classification algorithms, offers a better classification performance. For the classification of multimodal MR images, we are using statistical as well as texture features. The following is a brief description of these features.

### 3.2.1 Statistical features

Statistical features are extracted using two techniques. The first is based on a first-order histogram, and the second referred to as a second-order statistical feature is based on the co-occurrence matrix. For this study, six first-order and seven second-order statistical features are used. This results in a total of 52 statistical features using all four MRI modalities. The statistical information of the image is referred to as the histogram of the image [23]. Probability density ($D$) is a measure of the intensity-level occurrence; this is obtained through the division of intensity-level histogram values ($I$) by the total number of pixels as shown in Eq. 1:

$$D(i) = \frac{I(m)}{HV}, m = 0, 1, \ldots.., G - 1 \quad (1)$$

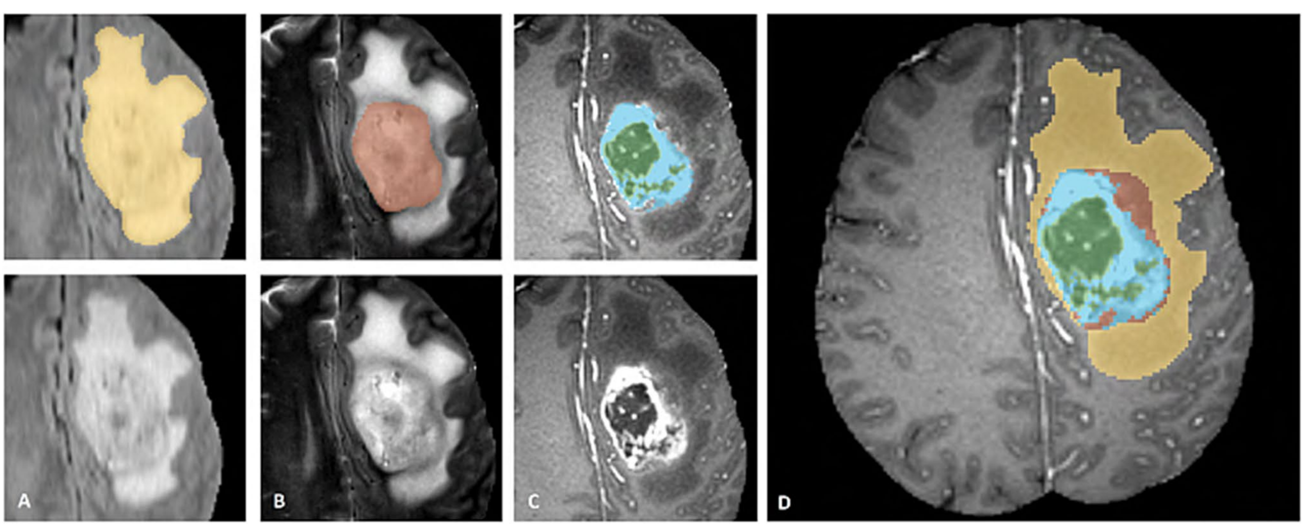


**Fig. 3** Sample of multiclass glioma labels with different tumor types. The image label shows **A** whole tumor, **B** tumor core, **C** enhancing tumor, and **D** combined all tumor types [22]

$H$ refers to the horizontal spatial domain resolution cells, and $V$ is the vertical spatial domain resolution cells. The variable $G$ represents the gray levels of the input MR image. Useful quantitative first-order statistical features are obtained from the image histogram. These features include the (i) mean, which measures the average of the intensity of the MR image; (ii) variance, which measures intensity variations around the mean; (iii) skewness, which measures the degree of asymmetry around the mean value of the histogram; (iv) kurtosis, which is a measure of histogram sharpness (v) energy, which measures histogram uniformity; and (vi) entropy, which measures the randomness of the distribution [24, 25].

The features extracted from the first-order statistics offer information about the gray-level distribution of MRI images. They do not offer any insights into the relative positions of different gray levels in MRI images. The co-occurrence matrix, which has second-order statistics, can help in extracting spatial information. The second-order features that are extracted using the co-occurrence matrix include (vii) angular second moment (ASM); (viii) correlation; (ix) inertia; (x) absolute value; (xi) inverse difference; (xii) entropy; and (xiii) maximum probability which can be calculated using Eq. 2 to Eq. 8, respectively:

$$S_{vii} = \sum_{m=0}^{G-1}\sum_{n=0}^{G-1}[D(m,n)]^2 \tag{2}$$

$$S_{viii} = \sum_{m=0}^{G-1}\sum_{n=0}^{G-1}\frac{m.n.D(m,n) - \mu_x\mu_y}{\sigma_x\sigma_y} \tag{3}$$

$$S_{ix} = \sum_{m=0}^{G-1}\sum_{n=0}^{G-1}(m-n)^2.D(m,n) \tag{4}$$

$$S_x = \sum_{m=0}^{G-1}\sum_{n=0}^{G-1}|m-n|.D(m,n) \tag{5}$$

$$S_{xi} = \sum_{m=0}^{G-1}\sum_{n=0}^{G-1}\frac{D(m,n)}{1+(m-n)^2} \tag{6}$$

$$S_{xii} = -\sum_{m=0}^{G-1}\sum_{n=0}^{G-1}D(m,n).\log_2 D(m) \tag{7}$$

$$S_{xiii} = \max_{m,n}(D(m,n)) \tag{8}$$

#### 3.2.2 Discrete wavelet transform features

In terms of cost and computation, DWT is considered a more efficient process [26]. Image texture can be analyzed using a wavelet used in image processing as a multi-resolution method. In this method, the third level decomposition is used to extract the wavelet features. Wavelet coefficients are used as feature vectors for the classification phase.

In the proposed method, DWT was also applied for 3 levels, and the top 100 features were selected. DWT decomposes the image into low- and high-frequency sub-bands called LL, LH, HL, and HH. LL is the low-frequency approximate of the input image that contains the most important features of the image and is used for further decomposition. LH and HL sub-band images give the horizontal and vertical features of the input image, respectively, and the HH sub-band image gives the diagonal features. In level 2, the same DWT was applied to the LL-decomposed image from level 1. The same process was repeated for level 3 DWT. Figure 4 shows the process model used for the DWT up to level 3 for the input MR image used to extract three-level DWT features. Daubechies 1 wavelet was used for the decomposition of the image at each level. The Daubechies 1 wavelet works based on the Haar filters [27]. The wavelet transform function $V$ of a continuous signal $x$ computes wavelet atoms by scaling and translating mother atoms as shown in Eq. 9 [28]:

$$V_{j,n}(x) = \frac{1}{2^j}v\left(\frac{x-2^j n}{2^j}\right) \tag{9}$$

The wavelet transform utilizes filters H and G represented in Eq. 10 and Eq. 11, respectively:

$$G(n) = \frac{1}{\sqrt{2}}(V\left(\frac{x}{2}\right), \partial(x-n)) \tag{10}$$

$$H(n) = \frac{1}{\sqrt{2}}(\partial\left(\frac{x}{2}\right), \partial(x-n)) \tag{11}$$

Based on Eq. 3 and Eq. 4, the simplest filter Daubechies 1 is based on the Harr filters in the form of $G = ([-1, 1])/\sqrt{2}$ and $H = ([1, 1])/\sqrt{2}$.

### 3.3 Classification techniques

We now present a concise background about the machine learning (ML) classifiers which help us in distinguishing among the various types of glioma tumors. Generally speaking, they are algorithms that take as input, the various features (labeled data) extracted from the MRI images (as described in the Proposed Work section) to learn a model. This learned model is further utilized for predicting the target variable (in our case, any of the four types of glioma tumors). Such ML algorithms are termed supervised classifiers. In this paper, we have used four different types of supervised classifiers, which are support vector machines (SVM),

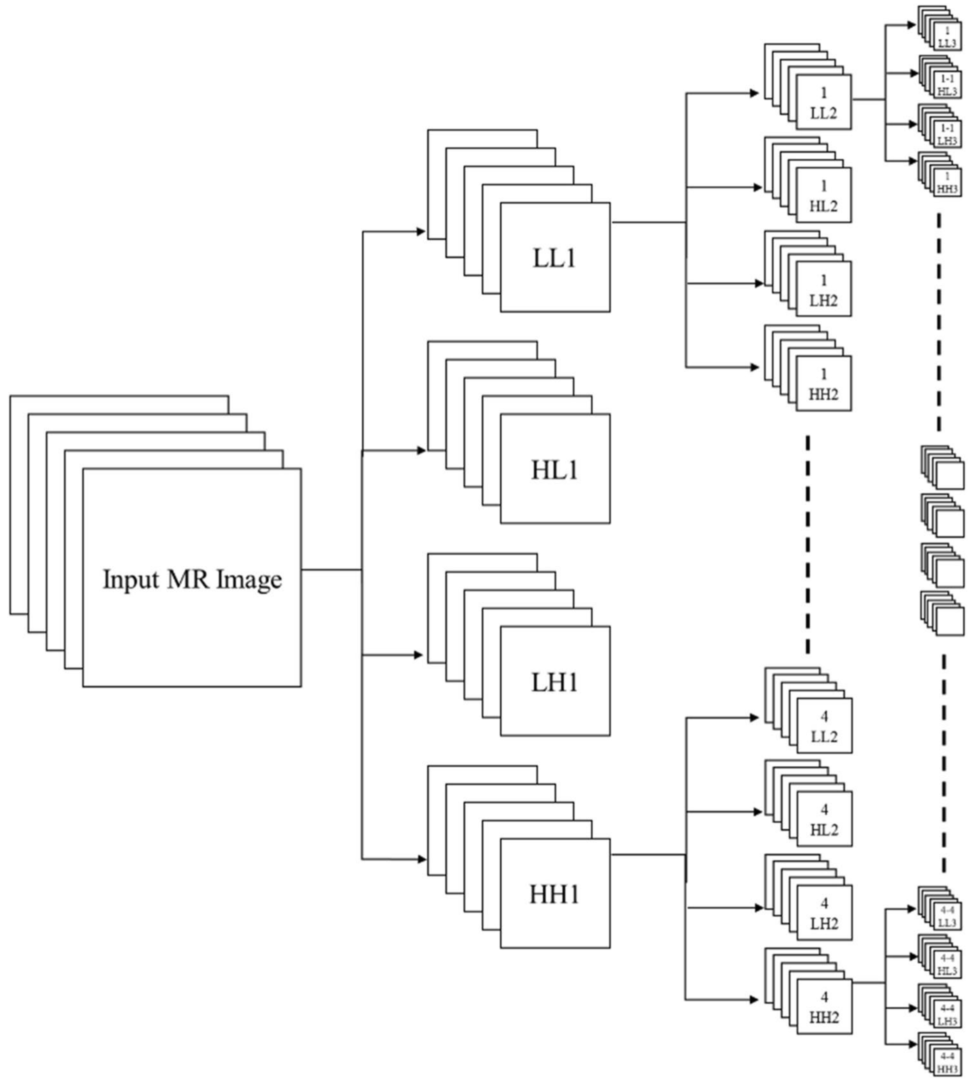


**Fig. 4** A process model of DWT up to level 3 that is used for extracting MR image features

random forest (RF), multilayer perceptron (MLP), and naïve Bayes (NB). The choice of using these classifiers is based on various criteria such as robustness (SVM), higher accuracy (RF), generality (MLP), and simplicity (NB) [29–31]. The proposed combined texture and statistical features are used as an input for these selected classifiers.

#### 3.3.1 Support vector machines (SVM)

Support vector machines (SVM) are actually a mathematical extension of neural networks which has the ability to classify linear as well as non-linear data. The way SVM implements the classification task is by transforming the input training data into multidimensional space and constructing hyperplanes in higher dimensions [32]. These hyperplanes are nothing but decision planes that aid in distinguishing a specific group of data from the other types. SVM essentially makes a search of those vector points in the space (referred to as support vector) which define the decision boundary that can provide a large separation between the existing classes. To implement the non-linear mapping of higher dimensional data, SVM uses what is called kernel functions, which are actually mathematical models. Some of the popular kernel functions include linear, polynomial, sigmoid, Gaussian, and radial basis. These kernel functions differ in their mathematical complexity, efficiency, and accuracy during the training and classification phases. It is observed that SVM has better generalization capability as compared to other classification approaches, and hence, they are used in situations where the number of training samples is less than the number of features in the dataset.

#### 3.3.2 Random forest classifier

Random forests are a type of classifiers that are termed ensemble learning classifiers. Such classifiers generate many classifiers and aggregate the results of their constituents. This results in better prediction accuracy and performance as compared to the one where a single classifier is employed [33]. Bagging and boosting are two popular methods used for implementing ensemble classifiers using decision trees (DT). Boosting is a recursive process of using multiple DTs to successively improve classification accuracy. However, in the bagging process, the constituent DTs independently make classification decisions, and the final result is achieved through majority voting. In RFs, the bagging process involves an extra layer of randomness where instead of choosing the predictor with the best split at each node, a predictor variable is chosen randomly from a subset of good predictors at each node. Due to this inherent randomness in the prediction process, RF has the ability to circumvent the problem of overfitting and generalize much better than other classification algorithms.

#### 3.3.3 Multilayer perceptron neural network (MLP)

A multilayer perceptron (MLP) is a feed-forward neural network (NN) consisting of different types of layers [34]. Essentially, it consists of the input layer, the hidden layer, and the output layer, consisting of a set of neurons (similar to the structure of the human brain). The data is given as input to the input layer, which actually implements a linear function. The hidden and output layers are designed to implement a non-linear function so as to model the data which is not linearly separable. Hence, MLPs are suitable for classifying data that inherently cannot be dealt with using linear function decision algorithms (e.g., linear regression). One of the popular non-linear activation functions is the sigmoid function which is used in the MLP. However, recently researchers have also used ReLU (rectified linear unit) in deep learning-based neural networks. The important property of MLP is that the neurons of the subsequent hidden layers are fully connected with certain weights. During the training process, the MLP layers start off with random weights, and these weights are iteratively updated based on the input data received in the training set. The weights are fine-tuned based on predicted output compared to the expected output. The backpropagation algorithm is used for this purpose. MLPs are widely applied to speech recognition and computer vision domains for the classification of various types of data.

#### 3.3.4 Naïve Bayes

NB classifier belongs to the supervised machine learning algorithms which work on the basic concept of the Bayes theorem [35]. NB owes its popularity to the simplicity of the mathematical modelling involved and its reasonable performance in terms of prediction accuracy in the classification tasks. In the abstract sense, the NB implements a conditional probability model where a data instance to be classified consists of a set of features. Given the observation (input data), the probability of predicting an output (the desired target variable) depends on the prior probability, the probability of observing the various data instances for the given hypothesis (conditional probability), and the observed data itself. One inherent drawback of the NB is that it assumes that features which define the input data (and the target variable) are statistically independent of each other. Even though this assumption simplifies the NB model mathematically, it also has an effect on its prediction accuracy. In spite of this weakness, NB is suitable in situations where the training data is scarce, and it still provides reasonable classification accuracy.

## 4 Experimental results

As described in the proposed Methodology section, DWT and statistical features are extracted from MR images of the MICCAI BraTS dataset. The significance of extracted features is studied using time tested machine learning approaches RF, SVM, MLP, and NB. The proposed methodology is applied to two glioma types LGG and HGG samples independently and tested for:

- Individual modality performance using mixed statistical and DWT feature sets
- Combined modalities using statistical, DWT feature sets, and mixed feature sets

The accuracy of classification is used as the main metric for performance measurement. Further, other metrics such as precision, recall, and F1-score are also measured to understand the reliability of the results. Accuracy is measured as the fraction of correct classifications. The metric recall measures the fraction of actual positive tumors classified. The metric precision measures the fraction of positive tumor classifications that are actually correct. Similarly, F1-score is the harmonic mean of precision and recall values. For each classifier, the experiments are executed for different parameters and are tuned for better accuracy. For easy comprehension, the results are discussed using the accuracy metric. Nonetheless, similar trends can be seen in the other metrics.

Table 1 shows the results obtained when applying the combined texture (DWT) and statistical features for each modality. For the HGG glioma type, RF achieved an average accuracy of 88.36% with the highest accuracy achieved in classifying the T1c modality. MLP achieved an average accuracy of 86.04%, and naïve Bayes achieved an average accuracy of 78.11%, while the SVM classifier used with a combined feature set achieved an average accuracy of 83.44% with Flair MR images.

**Table 1** Comparison of multiclass glioma tumor classification using combined DWT and statistical features for each MRI modality

| Glioma type | Classifier | Modality | Individual class accuracies | | | | Average measures | | | |
|---|---|---|---|---|---|---|---|---|---|---|
| | | | Necrosis | Edema | Non-enhancing | Enhancing | Acc | Precision | Recall | F measure |
| HGG | RF | Flair | 85.42 | 99.23 | 83.25 | 83.38 | 87.82 | 0.863 | 0.846 | 0.854 |
| | | T1 | 84.68 | 99.23 | 83.22 | 83.31 | 87.61 | 0.863 | 0.842 | 0.851 |
| | | T1c | 86.89 | 99.23 | 83.73 | 83.60 | 88.36 | 0.869 | 0.849 | 0.858 |
| | | T2 | 83.38 | 99.23 | 82.49 | 82.35 | 86.86 | 0.857 | 0.829 | 0.842 |
| | MLP | Flair | 80.50 | 99.23 | 82.14 | 81.05 | 85.73 | 0.849 | 0.815 | 0.831 |
| | | T1 | 80.47 | 99.23 | 81.28 | 80.22 | 85.30 | 0.834 | 0.821 | 0.827 |
| | | T1c | 82.58 | 99.23 | 81.15 | 81.21 | 86.04 | 0.841 | 0.830 | 0.835 |
| | | T2 | 78.97 | 99.23 | 79.90 | 80.06 | 84.54 | 0.847 | 0.777 | 0.809 |
| | SVM | Flair | 78.49 | 99.23 | 78.85 | 77.19 | 83.44 | 0.823 | 0.778 | 0.799 |
| | | T1 | 70.80 | 99.23 | 78.69 | 77.98 | 81.68 | 0.840 | 0.735 | 0.777 |
| | | T1c | 71.83 | 99.23 | 78.09 | 77.60 | 81.69 | 0.804 | 0.787 | 0.793 |
| | | T2 | 78.43 | 99.23 | 77.29 | 77.76 | 83.18 | 0.850 | 0.732 | 0.769 |
| | NB | Flair | 71.47 | 84.56 | 77.10 | 77.95 | 77.77 | 0.813 | 0.750 | 0.772 |
| | | T1 | 69.91 | 84.85 | 76.94 | 77.60 | 77.32 | 0.808 | 0.745 | 0.767 |
| | | T1c | 70.52 | 85.33 | 76.17 | 76.13 | 77.04 | 0.795 | 0.758 | 0.767 |
| | | T2 | 70.90 | 84.94 | 78.02 | 78.56 | 78.11 | 0.831 | 0.731 | 0.770 |
| LGG | RF | Flair | 85.10 | 99.30 | 84.11 | 81.56 | 87.52 | 0.864 | 0.850 | 0.857 |
| | | T1 | 85.23 | 99.30 | 83.73 | 81.68 | 87.49 | 0.866 | 0.845 | 0.854 |
| | | T1c | 86.06 | 99.30 | 84.43 | 81.11 | 87.72 | 0.869 | 0.847 | 0.857 |
| | | T2 | 81.62 | 99.30 | 83.32 | 79.83 | 86.02 | 0.857 | 0.825 | 0.839 |
| | MLP | Flair | 78.81 | 99.30 | 82.58 | 76.04 | 84.18 | 0.855 | 0.781 | 0.814 |
| | | T1 | 82.07 | 99.30 | 81.50 | 75.56 | 84.61 | 0.859 | 0.775 | 0.811 |
| | | T1c | 81.27 | 99.30 | 80.93 | 77.19 | 84.67 | 0.876 | 0.755 | 0.804 |
| | | T2 | 76.99 | 99.30 | 81.21 | 76.16 | 83.42 | 0.847 | 0.771 | 0.806 |
| | SVM | Flair | 76.39 | 99.30 | 80.26 | 73.13 | 82.27 | 0.795 | 0.827 | 0.809 |
| | | T1 | 76.74 | 99.30 | 80.57 | 73.87 | 82.62 | 0.833 | 0.767 | 0.793 |
| | | T1c | 76.90 | 99.30 | 80.22 | 73.80 | 82.56 | 0.813 | 0.798 | 0.801 |
| | | T2 | 75.23 | 99.24 | 78.49 | 72.69 | 81.41 | 0.794 | 75.478 | 0.773 |
| | NB | Flair | 70.13 | 85.42 | 77.07 | 73.74 | 76.59 | 0.816 | 0.733 | 0.763 |
| | | T1 | 69.46 | 85.71 | 75.69 | 74.12 | 76.25 | 0.809 | 0.735 | 0.761 |
| | | T1c | 70.01 | 87.37 | 75.60 | 73.87 | 76.71 | 0.807 | 0.743 | 0.764 |
| | | T2 | 68.92 | 86.57 | 77.61 | 74.31 | 76.85 | 0.830 | 0.716 | 0.759 |

For LGG glioma types, RF achieved an average accuracy of 87.52% with the highest accuracy achieved in classifying class 2. MLP achieved an average accuracy of 84.67%, and naïve Bayes achieved an average accuracy of 76.85%, while the SVM classifier used with a combined feature set achieved an average accuracy of 82.62%. RF has the best overall accuracy using combined texture (DWT) and statistical features for the different modalities. The highest average accuracy for RF for HGG glioma type T1c modality was 88.36% with a precision of 0.869, recall 0.849, and F measure 0.858, while for LGG RF achieved the highest average accuracy for the Flair modality of 87.52% with a precision of 0.864, recall of 0.850, and F measure of 0.857.

Figure 5 shows a visual representation of the data obtained in Table 1. It is clear from the figure that RF was able to achieve the highest accuracies overall for all of the modalities. The visual representation shows that MLP achieves the second highest accuracies after RF and that the lowest accuracies are achieved when using NB.

Table 2 shows the results obtained using combined texture (DWT) and statistical features combining all modalities: Flair, T1, T1c, and T2. To test and analyze the effectiveness of combining the texture (DWT) and statistical features, the experiment was separated into three phases: (1) combining modalities with DWT features only, (2) combining modalities with statistical features only, and (3) combining modalities with combined

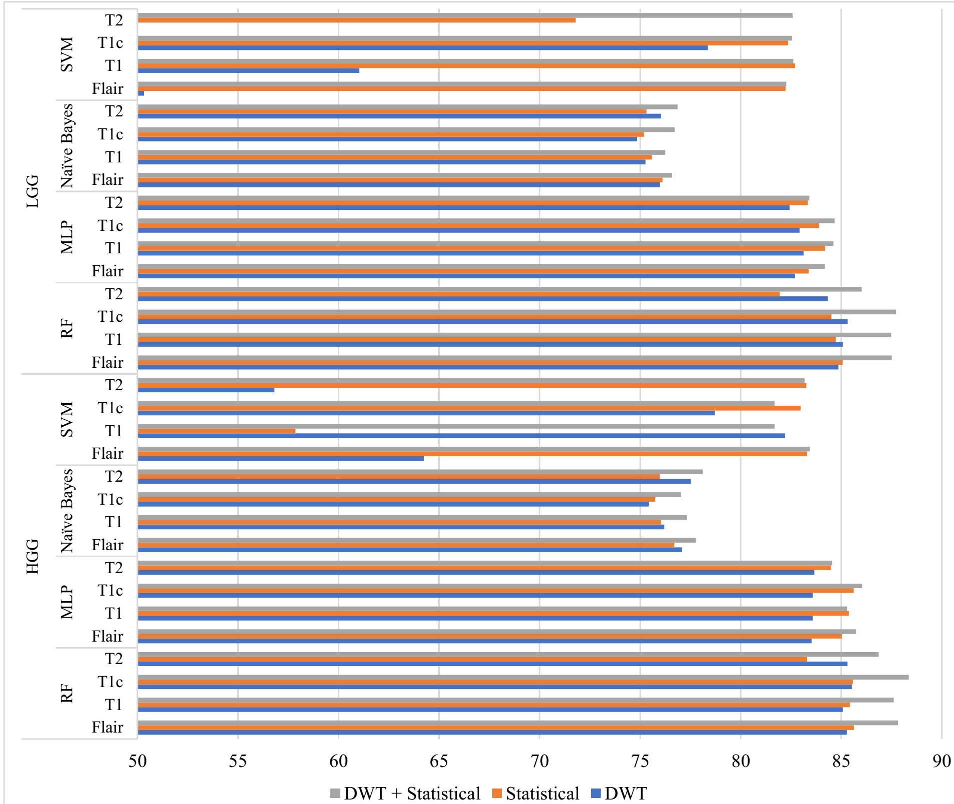


**Fig. 5** Comparison of averages accuracies for multiclass glioma classification using hybrid DWT and texture features

DWT and statistical features. With the combined DWT and statistical features, the RF classifier achieved the highest overall average classification accuracy of 89.59% for Flair MR images of the HGG modalities. This was the same for the LGG glioma type as RF displayed better accuracy than the rest of the classifiers with an average accuracy of 90.28%.

When using statistical features only for all modalities combined, the RF, MLP, and SVM classifiers achieve results within the same range. However, RF showed a slight improvement with combined texture and statistical features for the combined modalities with an average accuracy of 89.59% for HGG and 90.28% for LGG as compared to an average highest accuracy of 88.36% and 87.52% for HGG and LGG from Flair MRI modality shown in Table 1. RF displayed improvement also when using combined DWT and statistical features for all modalities. For both HGG and LGG, a significant improvement of 1.23% and 2.76% has been noticed, respectively, with combined features and combined modalities. The main reason for getting better accuracies for multiclass glioma tumor classification with RF is that it is a bagging algorithm that can avoid overfitting. RF is an ensemble-based method; thus, it works better with a small feature set of tumorous images. RF is a combination of multiple decision trees, which partition the training set into small subsets until it reaches the class uniform. This local learning approach of RF is very effective for the characterized data by multiple clusters dispersed over the feature space.

Figure 6 shows a visual representation of the data obtained in Table 2. It is clear from the figure that RF was able to achieve the highest accuracies overall for all of the modalities. The visual representation shows that MLP achieves the second highest accuracies after RF and that the lowest accuracies are achieved when using NB.

## 5 Discussions

The proposed combined DWT and statistical feature sets are used to classify the four classes of glioma tumors of HGG and LGG types. After feature extraction, typical classifiers such as RF, naïve Bayes, SVM, and MLP were used, and accuracy-based performance was compared. In the proposed method, combined DWT and statistical features from individual modalities were used with classifiers: RF, naïve Bayes, SVM, and MLP. The best accuracy results were achieved when used with RF classifier, as shown in Table 1. For the HGG glioma type, the best average accuracy of 88.36% was achieved with the RF classifier. While using the MLP classifier, the average accuracy was better but still less than RF for most of the classes, ranging from 84.54 to 86.04%. SVM and

**Table 2** Comparison of multiclass glioma classification using combined texture and statistical features for combined all modalities

| Glioma type | Feature type | Classifier | Individual class accuracies | | | | Average measures | | | |
|---|---|---|---|---|---|---|---|---|---|---|
| | | | Necrosis | Edema | Non-enhancing | Enhancing | Acc | Precision | Recall | F measure |
| HGG (merged modalities) | DWT features | RF | 86.31 | 99.2 | 83.16 | 83.5 | 88.04 | 0.867 | 0.843 | 0.854 |
| | | MLP | 79.9 | 99.23 | 80.77 | 80.92 | 85.21 | 0.842 | 0.817 | 0.828 |
| | | SVM | 68.99 | 46.41 | 24.4 | 43.71 | 45.88 | 0.579 | 0.714 | 0.581 |
| | | NB | 69.08 | 84.53 | 76.97 | 76.9 | 76.87 | 0.813 | 0.722 | 0.758 |
| | Statistical features | RF | 85.61 | 99.27 | 83.73 | 81.62 | 87.56 | 0.877 | 0.878 | 0.878 |
| | | MLP | 79.93 | 99.3 | 82.01 | 77.95 | 84.80 | 0.863 | 0.837 | 0.848 |
| | | SVM | 70.07 | 91.77 | 28.9 | 69.18 | 64.98 | 0.782 | 0.829 | 0.805 |
| | | NB | 68.57 | 85.3 | 77.07 | 73.39 | 76.08 | 0.750 | 0.833 | 0.778 |
| | DWT and statistical features | RF | 88.65 | 99.2 | 85.04 | 85.45 | 89.59 | 0.885 | 0.880 | 0.882 |
| | | MLP | 85.71 | 99.23 | 83.09 | 81.84 | 87.47 | 0.846 | 0.849 | 0.847 |
| | | SVM | 75.49 | 99.23 | 77.29 | 76.83 | 82.21 | 0.794 | 0.837 | 0.815 |
| | | NB | 75.14 | 85.49 | 71.87 | 72.69 | 76.30 | 0.817 | 0.748 | 0.773 |
| LGG (merged modalities) | DWT features | RF | 88.29 | 99.33 | 84.5 | 83.95 | 89.02 | 0.868 | 0.842 | 0.853 |
| | | MLP | 84.11 | 99.33 | 83.22 | 79.26 | 86.48 | 0.851 | 0.801 | 0.820 |
| | | SVM | 77.47 | 99.3 | 81.34 | 73.93 | 83.01 | 0.669 | 0.759 | 0.687 |
| | | NB | 75.24 | 87.46 | 71.77 | 70.49 | 76.24 | 0.822 | 0.709 | 0.752 |
| | Statistical features | RF | 89.25 | 99.2 | 86.06 | 86.25 | 90.19 | 0.877 | 0.866 | 0.871 |
| | | MLP | 82.67 | 99.23 | 82.26 | 82.77 | 86.73 | 0.865 | 0.821 | 0.842 |
| | | SVM | 78.02 | 99.23 | 78.21 | 78.27 | 83.43 | 0.815 | 0.811 | 0.811 |
| | | NB | 71.06 | 85.42 | 77.48 | 78.17 | 78.03 | 0.753 | 0.841 | 0.783 |
| | DWT and statistical features | RF | 89.25 | 99.3 | 86.57 | 85.99 | 90.28 | 0.892 | 0.883 | 0.887 |
| | | MLP | 80.03 | 99.3 | 82.2 | 81.49 | 85.76 | 0.866 | 0.805 | 0.832 |
| | | SVM | 69.5 | 99.3 | 80.51 | 69.66 | 79.74 | 0.861 | 0.683 | 0.750 |
| | | NB | 70.55 | 86.92 | 77.07 | 74.79 | 77.33 | 0.823 | 0.736 | 0.768 |

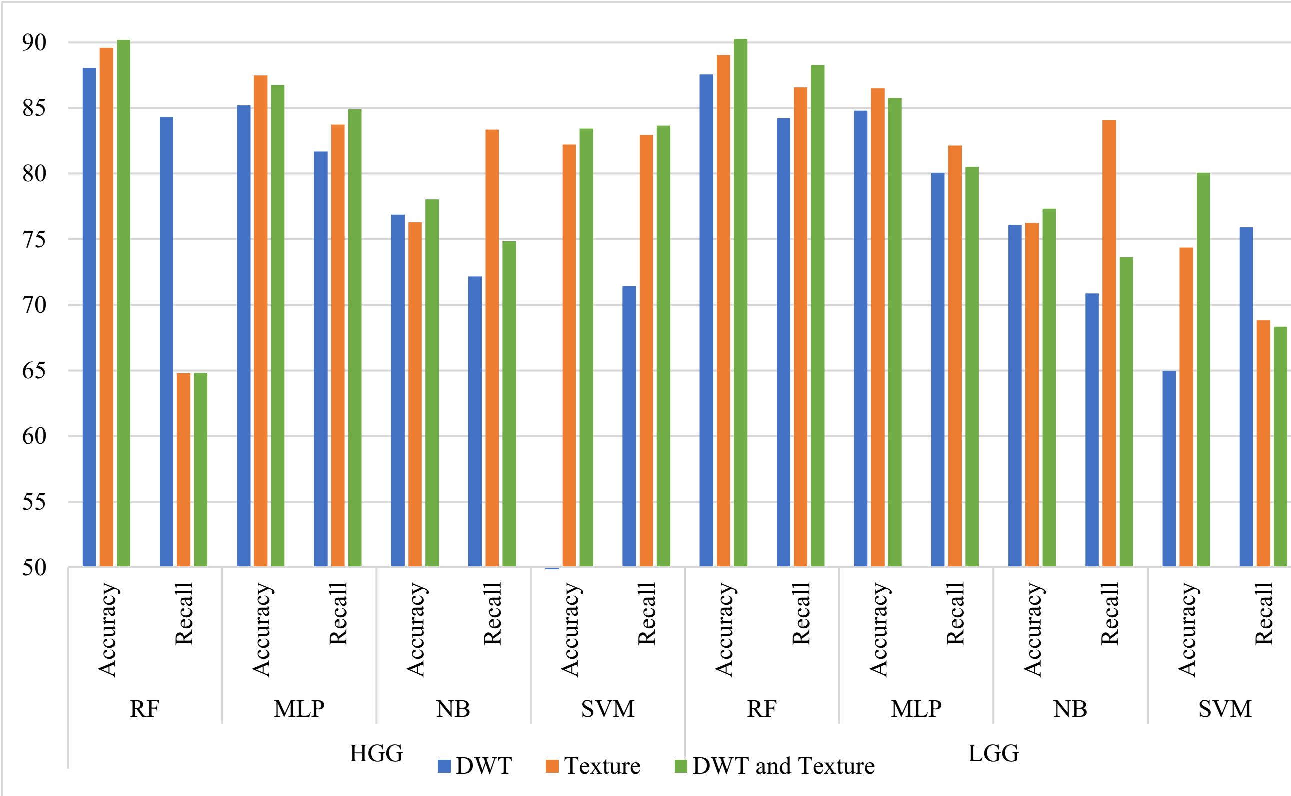


**Fig. 6** Comparison of accuracies glioma classification using hybrid features for combined all modalities

naïve Bayes secured an almost similar kind of accuracy range for all classes but less than RF and MLP as shown in Table 1. Although the naïve Bayes classifier is simple to implement and faster, it is feature-independent for the prediction of the probability of the class as observed in brain MR images. Different types of glioma tumor pixels in the MR image are highly correlated due to the complex nature of glioma tumor tissues and brain cells, so the features also have a high correlation. Similar kinds of results were observed when LGG glioma is classified, where again the highest average accuracy was achieved when the RF classifier was used, achieving 87.52%. From the statistical analysis presented in Table 2, it can be stated that RF has the best overall accuracy using combined DWT and statistical features for each modality which is moderately better than MLP and other classifiers. In Table 2, the classification results were combined for all MRI modalities: Flair, T1, T1c, and T2. These results were compared for three scenarios. First, only DWT features were used with combined modalities, and in this case, overall highest accuracy range is secured if RF is used as a classifier for both HGG and LGG glioma types. In the second case where only statistical features were used with combined modalities again, RF secured the best averages, but it was close to SVM and MLP for both HGG and LGG glioma types. For the third case, both DWT and statistical features were combined and used which achieved a better accuracy of 89.59% and

**Table 3** Comparison of the proposed methods for multiclass glioma tumor classification with latest literature techniques

| Reference | Method | Data | Accuracy |
|---|---|---|---|
| | Proposed method (statistical + DWT, RF as classifier) | BraTS | 90.28% |
| El-Melegy & El-Magd (2019) [36] | Ten statistical features and random forest as classifier | BraTS | 80.85% |
| Xue et al. (2020) [37] | Dual path residual convolutional neural network | BraTS | 84.90% |
| Cho et al. (2018) [38] | ROI and radiomics features with ensemble classifier | BraTS | 89.47% |
| Cho et al. (2018) [38] | ROI and radiomics features with RF classifier | BraTS | 88.77% |

90.28% for HGG and LGG, respectively. From the statistical analysis presented in Table 1 and Table 2, it is concluded that the combination of DWT and statistical features with all modalities combined achieves the best accuracies using the RF classifier for both LGG an HGG.

As shown in Table 3, the proposed technique using combined DWT and statistical features with RF as a classifier achieved an accuracy of 90.28% for multiclass classification. When compared with other recent techniques from literature, it is evident that the proposed technique outperformed those listed in Table 3.

## 6 Conclusion

Brain tumors are one of the fatal diseases and can lead to death if not diagnosed early. The early diagnosis of brain tumors depends on the early symptoms and the early analysis of the brain MRI images by highly skilled professionals. The requirement of analysis of the brain images by highly skilled individuals makes it a costly and time-consuming process which means that the analysis cannot be done for everyone and only for patients who display early symptoms of cancer. In addition, insurance companies will not approve these tests for everyone due to the cost factor, but even with cost factor aside, skilled professionals have a certain capacity that they cannot exceed. Therefore, if an automated method can be developed with high accuracy of diagnosis, it may be better than the method performed by humans because processes performed by humans are prone to human errors. In this article, a method is proposed for feature extraction from the MRI images. In this method, we propose the combination of both textural features extracted using the DWT combined with statistical features using the first- and second-order statistical features. After a thorough comparison of using either the texture features and statistical features individually on individual modalities and the use of the features combined on combined modalities, the experimental results showed that the highest average accuracies were achieved using the combined features (both textural and statistical) on combined modalities. The random forest classifier outperformed the other classifiers in this study. The results show that the average accuracy using the RF classifier with combined features on combined modalities is 89.59% for HGG and 90.28% for LGG. This is higher than any similar method reported in recent literature. Future work will continue the process to improve the early automatic classification and diagnosis of glioma tumors to produce a system that can be applied in hospitals with high reliability. In addition, the authors are exploring the use of deep learning models for other medical conditions that may assist in the automatic diagnosis without human intervention.

## Declarations

**Conflict of interest** The authors declare no competing interests.

## References


1. Ker J, Bai Y, Lee HY, Rao J, Wang L (2019) Automated brain histology classification using machine learning. J Clin Neurosci 66:239–245
2. Pintelas E, Liaskos M, Livieris IE, Kotsiantis S, Pintelas P (2020) Explainable machine learning framework for image classification problems: case study on glioma cancer prediction. J Imaging 6(6):37
3. Van den Bent MJ (2010) Interobserver variation of the histopathological diagnosis in clinical trials on glioma: a clinician's perspective. Acta Neuropathol 120(3):297–304
4. Kumar S, Dabas C, Godara S (2017) Classification of brain MRI tumor images: a hybrid approach. Procedia Comput Sci 122:510–517
5. Lundervold AS, Lundervold A (2019) An overview of deep learning in medical imaging focusing on MRI. Z Med Phys 29:102–127
6. Zacharaki EI, Wang S, Chawla S, Soo Yoo D, Wolf R, Melhem ER, Davatzikos C (2009) Classification of brain tumor type and grade using MRI texture and shape in a machine learning scheme. Magn Reson Med 62:1609–1618
7. Jayachandran A, Kharmega Sundararaj G (2015) Abnormality segmentation and classification of multi-class brain tumor in MR images using fuzzy logic-based hybrid kernel SVM. Int J Fuzzy Syst 17:434–443
8. Bahadure NB, Ray AK, Thethi HP (2017) Image analysis for MRI based brain tumor detection and feature extraction using biologically inspired BWT and SVM. Int J Biomed Imaging 2017:9749108
9. Iqbal S, Khan M, Saba T, Rehman A (2018) Computer-assisted brain tumor type discrimination using magnetic resonance imaging features. Biomed Eng Lett 8(1):5–28
10. Sengupta A, Ramaniharan AK, Gupta RK, Agarwal S, Singh A (2019) Glioma grading using a machine-learning framework based on optimized features obtained from T1 perfusion MRI and volumes of tumor components. J Magn Reson Imaging 50:1295–1306
11. Gupta N, Bhatele P, Khanna P (2019) Glioma detection on brain MRIs using texture and morphological features with ensemble learning. Biomed Signal Process Control 47:115–125
12. Gilanie G, Bajwa UI, Waraich MM, Habib Z (2019) Computer aided diagnosis of brain abnormalities using texture analysis of MRI images. Int J Imaging Syst Technol 29(3):260–271
13. Bhatele KR, Bhadauria SS (2021) Machine learning application in glioma classification: review and comparison analysis. Arch Comput Methods Eng 1–28
14. Jena B, Nayak GK, Saxena S (2022) An empirical study of different machine learning techniques for brain tumor classification and subsequent segmentation using hybrid texture feature. Mach Vis Appl 33(1):1–16
15. Öksüz C, Urhan O, Güllü MK (2022) Brain tumor classification using the fused features extracted from expanded tumor region. Biomed Signal Process Control 72:103356
16. Latif G, Butt MM, Khan AH, Butt MO, Al-Asad JF (2017) Automatic multimodal brain image classification using MLP and 3D glioma tumor reconstruction. In: 2017 9th IEEE-GCC Conference and Exhibition (GCCCE). IEEE, pp 1–9
17. Latif G, Butt MM, Khan AH, Butt O, Iskandar DA (2017) Multiclass brain Glioma tumor classification using block-based 3D wavelet features of MR images. In: 2017 4th International

Conference on Electrical and Electronic Engineering (ICEEE). IEEE, pp 333–337
18. Sharif MI, Li JP, Khan MA, Saleem MA (2020) Active deep neural network features selection for segmentation and recognition of brain tumors using MRI images. Pattern Recogn Lett 129:181–189
19. Deepak S, Ameer PM (2021) Automated categorization of brain tumor from MRI using CNN features and SVM. J Ambient Intell Humaniz Comput 12(8):8357–8369
20. Kang J, Ullah Z, Gwak J (2021) MRI-based brain tumor classification using ensemble of deep features and machine learning classifiers. Sensors 21(6):2222
21. Tripathi PC, Bag S (2022) A computer-aided grading of glioma tumor using deep residual networks fusion. Comput Methods Programs Biomed 215:106597
22. Weninger L, Rippel O, Koppers S, Merhof D (2018) Segmentation of brain tumors and patient survival prediction: methods for the brats 2018 challenge. In: International MICCAI brainlesion workshop. Springer, Cham. pp 3–12
23. Bharati MH, Liu JJ, MacGregor JF (2004) Image texture analysis: methods and comparisons. Chemom Intell Lab Syst 72(1):57–71
24. Qurat-Ul-Ain GL, Kazmi SB, Jaffar MA, Mirza AM (2010) Classification and segmentation of brain tumor using texture analysis. In: 9th WSEAS International conference on artificial intelligence, knowledge engineering and data bases. pp 147–155
25. Pushpa BR, Louies F (2019) Detection and classification of brain tumor using machine learning approaches. Int J Res Pharm Sci 10(3):2153–2162
26. Nilesh B, Sachin S, Pradip N, Rane DB (2013) Image compression using discrete cosine transform and discrete wavelet transform. Int J Comput Technol Electron Eng 3(11):54–59
27. Ullah Z, Lee SH, Fayaz M (2019) Enhanced feature extraction technique for brain MRI classification based on Haar wavelet and statistical moments. Int J Adv Appl Sci 6(7):89–98
28. Islam M, Roy A, Laskar RH (2020) SVM-based robust image watermarking technique in LWT domain using different subbands. Neural Comput Appl 32(5):1379–1403
29. Subudhi A, Dash M, Sabut S (2020) Automated segmentation and classification of brain stroke using expectation-maximization and random forest classifier. Biocybernet Biomed Eng 40(1):277–289
30. Sidike P, Asari VK, Sagan V (2018) Progressively expanded neural network (PEN Net) for hyperspectral image classification: a new neural network paradigm for remote sensing image analysis. ISPRS J Photogramm Remote Sens 146:161–181
31. Salman SAB, Salih AHA, Ali AH, Khaleel MK, Mohammed MA (2018) A new model for iris classification based on naïve Bayes grid parameters optimization. Int J Sci: Basic Appl Res 40(2):150–155
32. Chandra MA, Bedi SS (2021) Survey on SVM and their application in image classification. Int J Inf Technol 13(5):1–11
33. Anitha R, Raja SS, D. (2018) Development of computer-aided approach for brain tumor detection using random forest classifier. Int J Imaging Syst Technol 28(1):48–53
34. Mataija M, Sablić-Nemec D (2021) Brain tumor detection based on MRI images using multilayer perceptron. Ri-STEM- 2021:95
35. Zaw HT, Maneerat N, Win KY (2019) Brain tumor detection based on naïve Bayes classification. In: 2019 5th International Conference on engineering, applied sciences and technology (ICEAST). IEEE, pp 1–4
36. El-Melegy MT, El-Magd KMA (2019) A multiple classifiers system for automatic multimodal brain tumor segmentation. In: Proceedings of the 15th International Computer Engineering Conference: Utilizing Machine Intelligence for a Better World. pp 58–63
37. Xue Y, Yang Y, Farhat FG, Shih FY, Boukrina O, Barrett AM, Binder JR, Graves WW, Roshan UW (2020) Brain tumor classification with tumor segmentations and a dual path residual convolutional neural network from MRI and pathology images. In: Lecture Notes in Artificial Intelligence and Lecture Notes in Bioinformatics. pp 360–367
38. Cho HH, Lee SH, Kim J, Park H (2018) Classification of the glioma grading using radiomics analysis. PeerJ 6:e5982



**Ghazanfar Latif** is a research coordinator (Deanship of Graduate Studies and Research) at Prince Mohammad Bin Fahd University, Saudi Arabia, and post-doctoral fellow at University of Quebec at Chicoutimi, Quebec, Canada. He holds a PhD degree from the University of Malaysia, Sarawak, Malaysia. He earned his MS degree in computer science from King Fahd University of Petroleum and Minerals, Saudi Arabia, in 2014 and BS degree in computer science from FAST National University of Computer and Emerging Sciences in 2010 by remaining in the dean's honor list. Throughout his educational carrier, he got a number of achievements like full scholarship for FSc, BS-CS, and MS-CS. He worked as an instructor at Prince Mohammad Bin Fahd University, Saudi Arabia, for 3 years in CS Department and has 2 years of industry work experience. His research interests include image processing, artificial intelligence, neural networks, and medical image processing.

**Abul Bashar** is currently working as assistant professor at Prince Mohammad Bin Fahd University, Kingdom of Saudi Arabia, in the College of Computer Engineering and Sciences. Earlier, he completed his PhD from the School of Computing and Information Engineering at the University of Ulster, Coleraine, UK, in 2011. He is a recipient of Osmania University Engineering Gold Medal in 1995, MS Research Scholarship from KFUPM (1996), and Vice Chancellors Research Scholarship from the University of Ulster (2008). He is actively involved in the TPC/review committees of renowned journals and conferences, namely, CSC IJCN, IEEE WCNC 2011, ISCI 2011, ICDIPC 2011, ICSECS 2011, DICTAP 2011, and NDT 2009/2010/2012.

**D. N. F. Awang Iskandar** is currently a senior lecturer at the Faculty of Computer Science and Information Technology (FCSIT), UNIMAS, Sarawak. She has a bachelor's degree (Hons) in information technology majoring in computational science, a master degree in multimedia computing, and a PhD in computer science. Currently, her research focuses on minimizing the gap between image features and high-level semantics in medical and agricultural content-based image retrieval systems. She has worked on techniques for querying an image collection including fusing text accompanying the images with visual features, automatic region tagging, and using ontology to enrich the semantic meaning of tagged image regions leading to the bridging of semantic gap in content-based image retrieval.

**Nazeeruddin Mohammad** completed his PhD from the School of Computing and Information Engineering at the University of Ulster, Coleraine, UK, in 2007. He received his Bachelor of Engineering (BE) degree in Electronics and Communications Engineering from Osmania University, India, in 1996. He has an MS degree in systems engineering from King Fahd University of Petroleum & Minerals (KFUPM), KSA, in 1999. He also received practical training and an Honours Diploma in Software Development from BDPS, India, in 1997. He is a recipient of MS Research Scholarship from KFUPM (1997), Vice Chancellors Research Scholarship from University of Ulster (2004), and first prize in the Faculty of Engineering Business Plan Competition at the University of Ulster (2006).

**Ghassen Ben Brahim** is an assistant professor of computer science at Prince Mohammed University. He received a PhD in computer science from Western Michigan University (USA). He worked as a systems analyst engineer at the Integrated Defense Systems of Boeing and as a research visitor at the US Naval Research Lab. His research interests include machine learning, computer and network security, wireless networks, QoS routing in large-scale MANETs, routing in all-optical networks, and the design and analysis of network protocols.

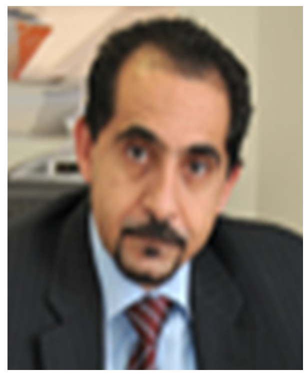

**Jaafar M. Alghazo** obtained his PhD and MSc in computer engineering from Southern Illinois University Carbondale in 2004 and 2000, respectively. He is currently working as LTC associate professor at Virginia Military Institute, Lexington, VA, USA. He joined Prince Mohammad Bin Fahd University (PMU) as founding dean of the College of Computer Engineering and Science and held various positions including Dean of Graduate Studies and Research, Dean of Institutional Relations, and Dean of Continuing Education and Community Service. Currently, he is assistant professor at PMU. His research interests include modelling and realization of biological mechanism using CAD and FPGAs, modelling and realization of arithmetic operations using CAD and FPGAs, low-power cache design, and assistive technology for students with disabilities.